Torque-Induced Change in Configuration of a Single NO Molecule on Cu(110)

Akitoshi Shiotari,[*] Takafumi Odani, and Yoshiaki Sugimoto
Department of Advanced Materials Science, The University of Tokyo, Kashiwa 277-8561, Japan

We demonstrated that a nitric oxide (NO) molecule on Cu(110) acts as an "ON-OFF-ON toggle switch" that can be turned on and off by repulsive force and electron injection, respectively. On the surface, NO molecules exist in three configurations: flat along the [001] direction (ON), upright (OFF), and flat along [00$\bar{1}$] (ON). An NO-functionalized tip, which was characterized by scanning tunneling microscopy and inelastic electron tunneling spectroscopy, can convert an upright NO adsorbate into a flat-lying NO. Atomic force microscopy and a simulation of the interactions between the NO molecules reveal that a repulsive force not aligned with the N—O bond provides the torque that detrudes the NO toggle; i.e., the upright NO adsorbate is tilted away from the tip. Therefore, the NO adsorbate behaves as a nonvolatile sensor for the detection of locally applied repulsive torque.

A molecule adsorbed on a surface or wedged between electrodes can act as a single-molecule switch if it has multiple stable or metastable configurations. Break-junction methods, scanning tunneling microscopy (STM), and atomic force microscopy (AFM) are commonly used to induce and fabricate single-molecule switches [1,2]. In particular, STM and AFM can provide local external stimuli from the tip to induce the switching of only one target molecule without interfering with other molecules located nearby. Voltage pulses have been heavily used as local stimuli from STM tips, which lead to configurational changes in the target molecule due to electron injection [3]. Furthermore, when the tip approaches a target molecule, interatomic attractive or repulsive forces between the tip and the sample can deform its molecular geometry, leading to switching of the configurations and/or electronic states [4–11]. AFM is the optimum method for evaluating the effect of tip-sample interactions on the geometries and motions of target adsorbates [12]. However, for large molecules and polyatomic clusters, the elementary processes responsible for tip-induced reactions involve multiple concerted interactions between the component atoms of the molecules, which complicate the interpretation of the experimental results; consequently, theoretical support is required. Unfortunately, experimental insight into the mechanical stimuli associated with STM and AFM tips is scarce and the underlying mechanism of the tip-induced reaction remains unknown.

Because of its simple structure, intensive investigations have elucidated the force responses between carbon monoxide (CO) adsorbates and probe tips [13–20]. It is well known that the tip can perturb the geometry of CO on a Cu surface [14–17]; however, an isolated CO adsorbate cannot act as a molecular switch because it only exists in one configuration on the surface. In contrast, nitric oxide (NO),

a diatomic molecule like CO, exists in several possible configurations on Cu(110) [21,22], making it an ideal system for investigating the mechanism of configurational change induced by external stimuli (e.g., heat, electrons, and mechanical force) because of its very simple molecular structure. Moreover, NO molecules adsorbed vertically on Cu surfaces have valence $2\pi^*$ states located at the Fermi level, which dominantly contribute to the tunneling current [23]. Therefore, the NO $2\pi^*$ orbital can be used to monitor the adsorption geometries of both the adsorbate and tip structures. In this Letter, we report that a NO molecule on Cu(110) can be detruded by repulsive rotational force from an NO-functionalized tip, in the same manner as turning on a macroscopic toggle switch.

STM and AFM experiments were carried out in an ultrahigh-vacuum chamber at 4.8 K [24]. STM images were acquired in constant-current mode with a sample bias V of 30 mV and a tunneling current I of 20 pA. Frequency-shift curves $\Delta f(z)$ were recorded using a qPlus force sensor [28] at $V = 0$ mV, and are displayed after subtracting $\Delta f(z)$ obtained over the bare Cu surface. The z origin was determined by STM over the bare surface. A positive (negative) z means that the tip was retracted from (pushed toward) the surface. The vertical force F_z and potential U were calculated from the $\Delta f(z)$ curves using the Sader formula [29].

As shown in Fig. 1(a), at submonolayer coverage, NO molecules on Cu(110) typically exist as three species: a monomer in an upright configuration bonded at the short-bridge site (upright NO), a monomer tilted largely in the [001] or [00$\bar{1}$] direction (flat-lying NO), and a dimer [(NO)$_2$] [21]. With a Cu tip, an upright NO is imaged as a dumbbell-shaped protrusion along the [1$\bar{1}$0] direction [Fig. 1(a), top]; this appearance reflects the $2\pi^*$ orbital
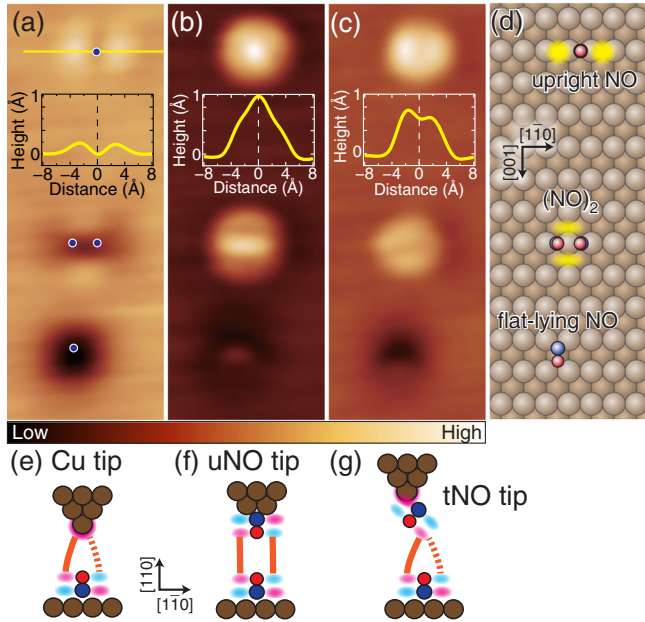
FIG. 1. (a)–(c) STM images of upright NO (top), $(NO)_2$ (middle), and flat-lying NO (bottom) on Cu(110) at 4.8 K with (a) Cu, (b) uNO, and (c) tNO tips. The blue dots in (a) represent the lateral positions of the N atoms. The insets depict line profiles measured over the upright NO along the yellow line in (a). (d) Atomic structure; the blue, red, and brown spheres represent N, O, and Cu atoms, respectively. The yellow lobes schematically represent the electron probability densities of the NO molecules near the Fermi level. (e)–(g) Side view schematic structures of an upright NO with (e) Cu, (f) uNO, and (g) tNO tips.

aligned in the $[1\bar{1}0]$ direction $[2\pi^*_{[1\bar{1}0]}$; Fig. 1(d), top] because the resonance state is localized at the Fermi level [21,30].

The interaction between the tip and the molecule on the surface depends on the structure of the tip apex [9,14,31]. Therefore, we varied the tip apex by extracting an upright NO molecule from the surface [24,32]. Two types of NO tips can be formed that can readily be distinguished by the STM appearances of the NO adsorbates. Figures 1(b) and 1(c) display STM images of the same area shown in Fig. 1(a) but acquired using different NO tips. Upright NO is observed as a round protrusion in the former image, whereas in the latter image it appears as a dumbbell-shaped protrusion with a larger apparent height than that observed with the Cu tip [Figs. 1(a)–1(c), inset]. Note that the three tip types were also distinguishable in the AFM images of the NO adsorbates [24]. The STM appearances of upright NO can be explained by the orbital distributions of the tip apices (s- and p-wave tip states [33,34]), based on Chen's derivative rule [35,36]. With the Cu tip (an s-wave tip), the $2\pi^*_{[1\bar{1}0]}$ orbital of NO on the surface is imaged as a dumbbell-shaped protrusion because the tunneling amplitudes from the two p-orbital lobes with opposite phases to the tip located just over the adsorbate cancel out [Fig. 1(e)].

On the other hand, a p-wave tip provides maximum tunneling amplitude when the tip is located over NO, which is consistent with the STM appearance [Fig. 1(b)]. Therefore, the corresponding tip is assigned to be an upright-NO tip (uNO tip) in which the NO $2\pi^*$ orbital ($2p_x$ and $2p_y$ of the O atom) dominates the tunneling process [Fig. 1(f)]. The STM appearance in Fig. 1(c) seems to directly reflect the orbital shapes of upright NO, as was observed for the s-wave tip. Therefore, we suggest that the NO molecule at the tip apex is tilted (tNO tip); consequently, one of the O 2p lobes behaves like a "p_z"-wave tip state [Fig. 1(g)]. The protruded lobe of the p orbital may be responsible for the higher image contrast than that observed with the s-wave Cu tip. The dumbbell shape of the upright NO observed with this tip is slightly asymmetric [Fig. 1(c), inset] probably because of the asymmetricity of the tip. These tip-structure assignments are fully supported by the STM appearances of $(NO)_2$ [Figs. 1(a)–1(d), middle] [37].

We assume that the NO-tip variety originates from several possible coordination numbers of NO at the tip apices. On Cu surfaces, the N atoms of NO molecules are coordinated to 2–4 Cu atoms [30,38]. When the tip apex consists of two or more Cu atoms [39,40], a uNO tip is expected to be preferably formed [Fig. 1(f)]. Moreover, in several Cu-nitrosyl complexes, NO bonded to a Cu atom is bent so as to effectively couple the NO $2\pi^*$ orbital to the Cu 4s and/or 3d orbitals [41–43]. Therefore, NO is possibly attached to the topmost Cu atom of the Cu tip, giving rise to a tNO tip [Fig. 1(g)]. In many cases, lifting an upright NO from the surface with a Cu tip results in a tNO tip [24], whereas it is difficult to controllably fabricate a uNO tip.

The round depression observed at the bottom in Fig. 1(a) is assigned to a flat-lying NO tilted in the [001] direction [Fig. 1(d), bottom], which is a more thermodynamically stable species than the upright molecule [21,22]. The submolecular structure appears in the STM images using both uNO and tNO tips [Figs. 1(b) and 1(c), bottom], where the bright lobe is ascribed to the approximate location of the O atom.

To determine the tip-apex structures, we conducted inelastic electron tunneling spectroscopy (IETS) [18]. The d^2I/dV^2 (dI/dV) spectrum recorded over the bare surface with a uNO tip exhibits a peak-and-dip (step) structure at $V = \pm 19$ mV [blue arrows in Fig. 2(a)]. This feature is almost identical to that observed in the spectrum recorded over an upright NO on Cu(110) with a Cu tip [24], which has been assigned to the frustrated translational mode along the $[1\bar{1}0]$ direction ($FT_{[1\bar{1}0]}$ mode; 18 meV) [30]. This clearly indicates that the NO molecule at the tip apex has a very similar bonding structure to that of upright NO on the Cu surface [Fig. 2(a), inset], which is consistent with the assignment based on its STM appearance (p-wave tip).

In contrast to the dI/dV spectrum for the uNO tip, dI/dV with the tNO tip is very different to that observed for
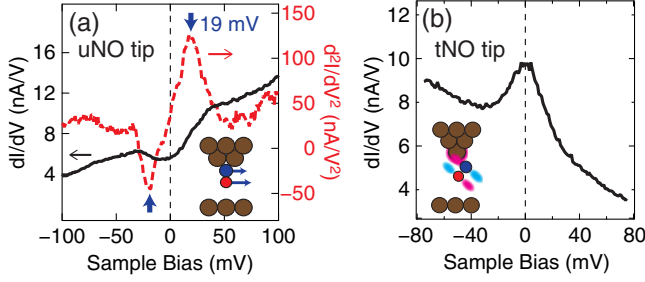
FIG. 2. (a) dI/dV (black) and d^2I/dV^2 (red) spectra recorded over the bare Cu(110) surface with a uNO tip. (b) dI/dV spectrum recorded over the bare surface with a tNO tip. Set point: $V = 30$ mV and $I = 200$ pA. The insets show side-view schematics of these systems.
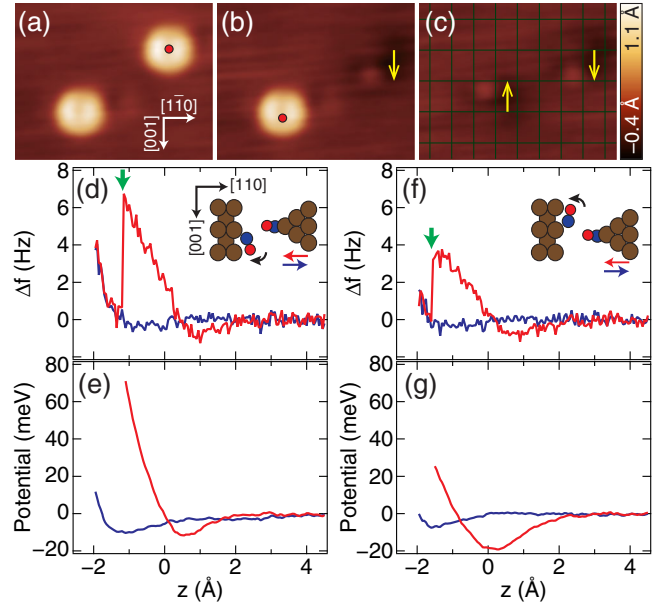

FIG. 3. Tip-induced conversion of upright NO into flat-lying NO. (a) STM images of two upright NO molecules on Cu(110) using a tNO tip. (b) The same area following approach of the tip to the surface over the red point in (a). (c) The same area after the tip approached the surface over the red point in (b). The green lines indicate the topmost Cu-atom lattice. (d) [(f)] $\Delta f(z)$ and (e) [(g)] $U(z)$ for (a) → (b) [(b) → (c)]. The tip approach and retraction are indicated in red and blue, respectively.

NO/Cu(110) with a Cu tip [24]; at the Fermi level, a sharp peak appears in the dI/dV recorded over the bare surface [Fig. 2(b)]. We assign this peak to NO $2\pi^*$ resonance states at the tip apex [24]. No IET signal was detected with this tip, supporting the observation that the NO-bonding structure at the tip apex differs substantially from that of upright NO and appears to be a tilted configuration [Fig. 2(b), inset].

We found that an NO tip induces the conversion of an upright NO molecule on the surface to the flat-lying configuration. The tilting direction (whether [001] or [00$\bar{1}$]) of the converted species can be controlled by changing the lateral position of the tip over the molecule (Fig. 3). When a tNO tip is displaced along the [00$\bar{1}$] ([001]) direction from the position directly over the upright NO, the vertical approach of the tip to the surface causes the target molecule to configurationally change into a flat-lying NO oriented in the [001] ([00$\bar{1}$]) direction as indicated by the yellow arrow in Fig. 3(b) [3(c)]. This means that upright NO molecules were detruded away from the tip. It is noteworthy that no bias voltage was applied during the tip-approach process; therefore, this reaction is not activated by electron injection, but by tip proximity. As was observed for the tNO tip, this configurational change was also induced by the approach of an oxygen-terminated tip [44] and a uNO tip [24]. In contrast, a Cu tip never induced this conversion because of the strong attractive force between the tip and the upright NO adsorbate, and the approach of the Cu tip eventually yields a NO tip, as described above. Therefore, we conclude that the application of repulsive force to the upright NO adsorbate plays a crucial role in activating this reaction. Inducing a configurational change in an individual NO molecule on Cu(110) corresponds directly to the controllable switching of molecular electronic states; the $2\pi^*$ valence orbital is localized on upright NO, whereas the $2\pi^*$ orbital of flat-lying NO is delocalized due to strong interactions with the Cu-substrate band [21].

The interaction between the NO adsorbate and the NO tip was investigated by AFM. Figures 3(d) and 3(f) show $\Delta f(z)$ curves recorded during the tip approach-and-retraction

processes that correspond to the transformations shown in Figs. 3(a) to 3(b) and 3(b) to 3(c), respectively. At far tip-sample distances, the Δf curves exhibit typical Lennard-Jones-potential-like features. In contrast, at $z \approx -1.5$ Å, the Δf signal dropped suddenly due to a change in configuration [green arrows in Figs. 3(d) and 3(f)]. The $U(z)$ curves [Figs. 3(e) and 3(g)] indicate that the configurational change occurred at a distance at which the repulsive force between the NO molecules begin to dominate ($U > 0$). However, the threshold values of U and F_z for this conversion depended on the lateral tip location [Figs. 3(e) and 3(g)] and the tip apex structure [24], which implies that values of U and F_z are not directly related to the conversion processes, but rather that an effective lateral force (i.e., repulsive torque) is required to tilt the upright NO adsorbate.

To confirm the importance of lateral repulsive force, we acquired $\Delta f(z)$ curves at several points along the [001] direction and display them as a two dimensional $U(x, z)$ map [Fig. 4(a)]; in the map the repulsive zone is localized at the top of the upright NO adsorbate [blue region in Fig. 4(a)] and is surrounded by a concentric attractive zone (red region). The appearance of this map is very similar to that observed for CO/Cu(111) with a CO tip [14], but in this case the configurational change of the adsorbate occurred at $(x, z) = (-0.2$ Å, -0.4 Å) [green line in Fig. 4(a)]. The force vectors $\boldsymbol{F}(x, z) = [-(\partial U/\partial x), -(\partial U/\partial z)]$ are distributed as shown by the black arrows in
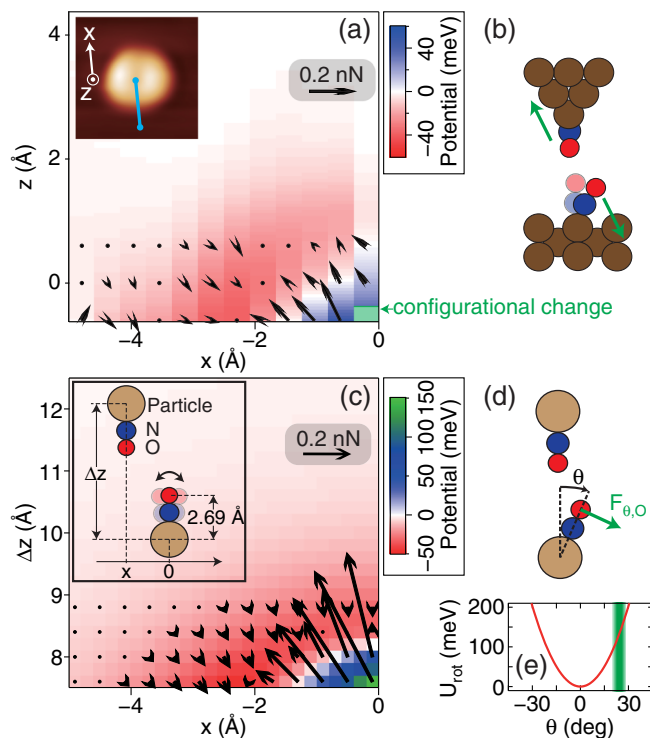
FIG. 4.   (a) $U(x, z)$ map recorded with a tNO tip near an upright NO on Cu(110). Inset shows an STM image of the target. The cyan line represents the x region of the map. Black arrows represent force vectors $\mathbf{F}(x, z)$ acting on the tip. Green line indicates the region where the NO configuration changes from upright to flat lying. (b) Depicting the side-view atomic structure immediately before conversion. (c) Simulated $U(x, \Delta z)$ map for a flexible NO adsorbate with a fixed NO molecule at the tip apex. Black arrows represent $\mathbf{F}(x, \Delta z)$ acting on the tip. Inset displays the model structure and the definitions of x and Δz. Brown spheres represent particles that simulate the surface and the tip body. (d) Model structure corresponding to $(x, \Delta z) = (-0.1\,\text{Å}, 7.6\,\text{Å})$, which is located at the bottom-right edge of the map. (e) Simulated potential surface for the rotation of the NO adsorbate.

Fig. 4(a), which represent the forces applied to the tip, and therefore, the adsorbate suffered counteractive forces. The force distribution indicates that, as well as vertical forces in the $-z$ direction, lateral forces in the $+x$ direction act on the NO adsorbate [green arrow in Fig. 4(b)] immediately prior to the change in configuration. Hence, we speculate that the lateral repulsive force induces the NO adsorbate to tilt in the opposite direction to the tip.

We reproduced the U map using a simple model analogous to that used in previous studies on CO/Cu(111) with a CO tip [15,39]. To model the tilting flexibility of the NO adsorbate, we applied a spring constant $\kappa = 2.4 \times 10^{-19}$ Nm for the rotation of NO around the bonding site, which was calculated from the FT$_{[001]}$ mode of NO/Cu(110) (6 meV) [30]. The energy to rotate the NO adsorbate was then calculated using a quadratic potential energy function: $U_{\text{rot}} = \frac{1}{2}\kappa\theta^2$ [Fig. 4(e)], where θ

is the NO tilt angle [Fig. 4(d)]. The Cu substrate and the tip body were simply modeled by two particles [Fig. 4(c), inset] and the tip-adsorbate interaction energy U_{tip} was described as the sum of the pairwise Lennard-Jones potentials [45,46]. At each tip position $(x, \Delta z)$, θ was determined so that the total potential $U_{\text{total}} = U_{\text{rot}} + U_{\text{tip}}$ was minimized. The remaining details of the calculational methods used are described in the Supplemental Material [24].

Figure 4(c) displays the calculated U map and $\mathbf{F}$ distribution. Cross-correlation matching of the experimental and simulated maps shows that $\Delta z = 8.1$ Å for this model corresponds to the experimental z origin [24]; therefore, the bottom-right edge of the simulation map is comparable to the point at which the configurational change was observed experimentally. At the tip position, θ was calculated to be $\sim 24°$ [Fig. 4(d)]. Then, the force perpendicular to the N—O bond of the adsorbate (F_θ) is about $+0.4$ nN for O [green arrow in Fig. 4(d)] and -0.01 nN for N, giving rise to a torque $\tau_{\text{NO}} \approx 1 \times 10^{-19}$ Nm that acts on the NO toggle [24]. Therefore, a repulsive force not aligned with the N—O bond, when applied to the O atom, provides sufficient torque to tilt the NO. At the tip position, U_{rot} was calculated to be 0.1–0.2 eV [green bar in Fig. 4(e)], by considering possible variations of the simulation parameters [24]. The activation energy E_a for the thermal reaction of upright NO to flat-lying NO is 0.125 eV [22], and therefore, the order of U_{rot} reasonably supports that the work done by the torque to tilt NO, which is equal to U_{rot}, decreases the activation energy eventually to zero [47]. We note that U_{rot} is calculated just under the harmonic approximation and that the reaction coordinate for configurational change is not considered in this simulation model. Evaluating the adsorption energies and reaction coordinate using the density functional theory would be helpful for gaining a theoretical understanding of the configurational transition. It is noteworthy that unlike U_{rot}, potential U obtained by force measurements [see Figs. 3(e), 3(g), and 4(a)] is *incommensurable* with respect to E_a because U includes interatomic interactions unrelated to the reaction. This may complicate the interpretation of the activation barrier for tip-induced reactions [13,16].

We did not observe the tip-induced backward reaction (flat to upright; $E_a = 0.170$ eV [22]), which is ascribed to the attractive force between the flat-lying NO and the tip being too small to overcome the backward-reaction barrier [blue curves in Figs. 3(e) and 3(g)]. As an alternative, electron injection can induce the one-way conversion of flat-lying NO to upright NO [21], which facilitates reversible switching with a NO tip [24].

In summary, we demonstrated that an NO molecule on Cu(110) works as an "ON-OFF-ON" toggle switch that is selectively turned on by a local mechanical stimulus. To turn on the NO switch, a tip that provides sufficient repulsive torque to rotate the NO adsorbate is required; therefore, the conversion of upright NO (OFF state) to

flat-lying NO (ON state) can be induced by "repulsive" NO tips but not by an "attractive" Cu tip. In contrast to the single-molecule *momentary* toggle switch reported previously [48], the ON state persists even after retraction of the tip, which indicates that the NO corresponds to a nonvolatile, *alternate-action* toggle switch. Therefore, the NO adsorbate behaves as a force sensor that memorizes the direction in which the repulsive force was applied; the used sensor can be "reset" (ON → OFF) by electron injection. The characteristic response of this simple molecule provides insight for the design of single-molecule machines with effective functions.

---

[*]shiotari@k.u-tokyo.ac.jp

[1] S. J. van der Molen and P. Liljeroth, J. Phys. Condens. Matter **22**, 133001 (2010).

[2] J. L. Zhang, J. Q. Zhong, J. D. Lin, W. P. Hu, K. Wu, G. Q. Xu, A. T. Wee, and W. Chen, Chem. Soc. Rev. **44**, 2998 (2015).

[3] B. C. Stipe, M. A. Rezaei, and W. Ho, Phys. Rev. Lett. **81**, 1263 (1998).

[4] C. Loppacher, M. Guggisberg, O. Pfeiffer, E. Meyer, M. Bammerlin, R. Lüthi, R. Schlittler, J. K. Gimzewski, H. Tang, and C. Joachim, Phys. Rev. Lett. **90**, 066107 (2003).

[5] A. Sweetman, S. Jarvis, R. Danza, J. Bamidele, S. Gangopadhyay, G. A. Shaw, L. Kantorovich, and P. Moriarty, Phys. Rev. Lett. **106**, 136101 (2011).

[6] R. Pawlak, S. Fremy, S. Kawai, T. Glatzel, H. Fang, L.-A. Fendt, F. Diederich, and E. Meyer, ACS Nano **6**, 6318 (2012).

[7] S. Yamazaki, K. Maeda, Y. Sugimoto, M. Abe, V. Zobač, P. Pou, L. Rodrigo, P. Mutombo, R. Pérez, P. Jelínek, and S. Morita, Nano Lett. **15**, 4356 (2015).

[8] W. Steurer, B. Schuler, N. Pavlicek, L. Gross, I. Scivetti, M. Persson, and G. Meyer, Nano Lett. **15**, 5564 (2015).

[9] J. N. Ladenthin, T. Frederiksen, M. Persson, J. C. Sharp, S. Gawinkowski, J. Waluk, and T. Kumagai, Nat. Chem. **8**, 935 (2016).

[10] Y. Zhang, Y. Wang, J.-T. Lü, M. Brandbyge, and R. Berndt, Angew. Chem. **56**, 11769 (2017).

[11] O. Stetsovych, P. Mutombo, M. Švec, M. Šámal, J. Nejedlý, I. Císařová, H. Vázquez, M. Moro-Lagares, J. Berger, J. Vacek, I. G. Stará, I. Starý, and P. Jelínek, J. Am. Chem. Soc. **140**, 940 (2018).

[12] O. Custance, R. Perez, and S. Morita, Nat. Nanotechnol. **4**, 803 (2009).

[13] M. Ternes, C. P. Lutz, C. F. Hirjibehedin, F. J. Giessibl, and A. J. Heinrich, Science **319**, 1066 (2008).

[14] Z. Sun, M. P. Boneschanscher, I. Swart, D. Vanmaekelbergh, and P. Liljeroth, Phys. Rev. Lett. **106**, 046104 (2011).

[15] A. J. Weymouth, T. Hofmann, and F. J. Giessibl, Science **343**, 1120 (2014).

[16] M. Emmrich, M. Schneiderbauer, F. Huber, A. J. Weymouth, N. Okabayashi, and F. J. Giessibl, Phys. Rev. Lett. **114**, 146101 (2015).

[17] Z. Han, G. Czap, C. Xu, C. L. Chiang, D. Yuan, R. Wu, and W. Ho, Phys. Rev. Lett. **118**, 036801 (2017).

[18] N. Okabayashi, A. Gustafsson, A. Peronio, M. Paulsson, T. Arai, and F. J. Giessibl, Phys. Rev. B **93**, 165415 (2016).

[19] A. Gustafsson, N. Okabayashi, A. Peronio, F. J. Giessibl, and M. Paulsson, Phys. Rev. B **96**, 085415 (2017).

[20] N. Okabayashi, A. Peronio, M. Paulsson, T. Arai, and F. J. Giessibl, Proc. Natl. Acad. Sci. U.S.A. **115**, 4571 (2018).

[21] A. Shiotari, Y. Kitaguchi, H. Okuyama, S. Hatta, and T. Aruga, Phys. Rev. Lett. **106**, 156104 (2011).

[22] A. Shiotari, T. Mitsui, H. Okuyama, S. Hatta, T. Aruga, T. Koitaya, and J. Yoshinobu, J. Chem. Phys. **140**, 214706 (2014).

[23] A. Shiotari, *Reactivity of Nitric Oxide on Copper Surfaces: Elucidated by Direct Observation of Valence Orbitals* (Springer, Singapore, 2017).

[24] See Supplemental Material at http://link.aps.org/supplemental/10.1103/PhysRevLett.121.116101 for details of experimental methods, STM and AFM images of NO/Cu(110) with Cu and NO tips, fabrication of the NO tip, IETS of NO/Cu(110) with Cu and NO tips, reversible switching of NO/Cu(110) with the tNO tip, configurational changes with uNO and O tips, and additional information for the experimental and simulated potential maps, which includes Refs. [25–27].

[25] R. Requist, S. Modesti, P. P. Baruselli, A. Smogunov, M. Fabrizio, and E. Tosatti, Proc. Natl. Acad. Sci. U.S.A. **111**, 69 (2014).

[26] V. Madhavan, W. Chen, T. Jamneala, M. F. Crommie, and N. S. Wingreen, Phys. Rev. B **64**, 165412 (2001).

[27] S. Liu, A. Shiotari, D. Baugh, M. Wolf, and T. Kumagai, Phys. Rev. B **97**, 195417 (2018).

[28] F. J. Giessibl, Rev. Mod. Phys. **75**, 949 (2003).

[29] J. E. Sader and S. P. Jarvis, Appl. Phys. Lett. **84**, 1801 (2004).

[30] A. Shiotari, H. Okuyama, S. Hatta, T. Aruga, M. Alducin, and T. Frederiksen, Phys. Rev. B **94**, 075442 (2016).

[31] G. Kichin, C. Wagner, F. S. Tautz, and R. Temirov, Phys. Rev. B **87**, 081408 (2013).

[32] H. Koshida, S. Hatta, H. Okuyama, A. Shiotari, Y. Sugimoto, and T. Aruga, J. Phys. Chem. C **122**, 8894 (2018).

[33] L. Gross, N. Moll, F. Mohn, A. Curioni, G. Meyer, F. Hanke, and M. Persson, Phys. Rev. Lett. **107**, 086101 (2011).

[34] M. Corso, M. Ondráček, C. Lotze, P. Hapala, K. J. Franke, P. Jelínek, and J. I. Pascual, Phys. Rev. Lett. **115**, 136101 (2015).

[35] C. J. Chen, Phys. Rev. B **42**, 8841 (1990).

[36] C. J. Chen, *Introduction to Scanning Tunneling Microscopy* (Oxford University Press on Demand, Oxford, England, 1993).

[37] With a Cu tip, the dimer is imaged as a shallow dumbbell-shaped protrusion along the [001] direction together with a central depression [Fig. 1(d), middle]; the highest occupied molecular orbital is mainly responsible for the shape of this protrusion. Therefore, an s-wave (p-wave) tip should provide an antinode (node) at the center of the dimer, which is in agreement with the STM appearance of $(NO)_2$ in Fig. 1(b) [1(c)].

[38] A. Shiotari, S. Hatta, H. Okuyama, and T. Aruga, J. Chem. Phys. **141**, 134705 (2014).

[39] J. Welker and F. J. Giessibl, Science **336**, 444 (2012).

[40] M. Emmrich, F. Huber, F. Pielmeier, J. Welker, T. Hofmann, M. Schneiderbauer, D. Meuer, S. Polesya, S. Mankovsky, D. Ködderitzsch, H. Ebert, and F. J. Giessibl, Science **348**, 308 (2015).

[41] W. Schneider, K. Hass, R. Ramprasad, and J. Adams, J. Phys. Chem. **100**, 6032 (1996).

[42] O. M. Usov, Y. Sun, V. M. Grigoryants, J. P. Shapleigh, and C. P. Scholes, J. Am. Chem. Soc. **128**, 13102 (2006).

[43] L. Wang, G. Wang, H. Qu, Z. H. Li, and M. Zhou, Phys. Chem. Chem. Phys. **16**, 10788 (2014).

[44] H. Mönig, D. R. Hermoso, O. Díaz Arado, M. Todorović, A. Timmer, S. Schüer, G. Langewisch, R. Pérez, and H. Fuchs, ACS Nano **10**, 1201 (2016).

[45] P. Hapala, G. Kichin, C. Wagner, F. S. Tautz, R. Temirov, and P. Jelínek, Phys. Rev. B **90**, 085421 (2014).

[46] P. Hapala, R. Temirov, F. S. Tautz, and P. Jelínek, Phys. Rev. Lett. **113**, 226101 (2014).

[47] A. L. Black, J. M. Lenhardt, and S. L. Craig, J. Mater. Chem. **21**, 1655 (2011).

[48] L. Gerhard, K. Edelmann, J. Homberg, M. Valášek, S. G. Bahoosh, M. Lukas, F. Pauly, M. Mayor, and W. Wulfhekel, Nat. Commun. **8**, 14672 (2017).